International Journal of Bifurcation and Chaos, Vol. 11, No. 11 (2001) 2881–2886

TRAVEL INSTABILITIES IN LATERAL HEATING

M. A. PELACHO, A. GARCIMARTÍN and J. BURGUETE
Departamento de Física y Matemática Aplicada,
Universidad de Navarra, E-31080 Pamplona, Spain

Received November 6, 2000; Revised January 22, 2001

We study the convective motion forced by lateral heating on a liquid layer. The movement is caused by two forces: buoyancy and thermocapillarity on the free surface, which is open to the air. As soon as a temperature gradient is imposed along the liquid layer, the fluid begins to move. When a certain threshold of the temperature difference is attained, this flow destabilizes and oscillations appear. We have performed an experiment to characterize the thermocapillary waves in a rectangular container whose dimensions can be continuously changed. This way, we are able to investigate how boundaries affect the threshold for the instability, as well as their consequences on other features of the waves.

1. Introduction

The convective motion generated in a fluid layer open to the air heated from the sides is not completely understood. A wide variety of instabilities rise up in this system depending on the value of several parameters: height of fluid h, horizontal temperature difference between the sides ΔT, value of the length l_x between these sides or l_y between the horizontal walls perpendicular to them, Pr Prandtl number of the fluid, Bi the Biot number, and so on. In the case of a very small fluid layer — typically one or two millimeters — subjected to a horizontal temperature difference, two forces appear which are responsible for the movement of the fluid: the surface tension σ and the buoyancy. As the temperature increases the surface tension decreases according to the law

$$\sigma(T) = \sigma(T_0) + \gamma(T - T_0)$$

γ being usually negative and T_0 a reference temperature. The density ρ of the fluid varies in the way

$$\rho(T) = \rho(T_0)[1 - \alpha(T - T_0)]$$

α being the thermal expansion coefficient. As a consequence, as soon as a temperature difference is imposed, the fluid begins to move, forming a basic flow which goes from the hot side (T_+) to the cold side (T_-) on the surface, and in the opposite sense at the bottom. For a bigger value of the temperature difference the basic flow destabilizes giving rise to a pair of hydrothermal waves that travel towards the hot side forming an angle with respect to the temperature gradient.

Such waves — *hydrothermal waves* — were predicted by Smith and Davis [1983] in their linear stability analysis. However, these authors did not consider the buoyancy forces but only the thermocapillary ones. In these conditions, the destabilization process was explained qualitatively by Smith [1986] some years later in terms of two different mechanisms depending on the value of the Prandtl number. Later, the works of Parmentier *et al.* [1993] and Mercier and Normand [1996] took into account the role of the gravity in the stability analysis. And thus other transitions were found when the basic flow destabilizes — steady and oscillatory modes, rolls and waves — as the thermocapillary forces dominate over the buoyancy or vice versa. These were observed in the experiments of Daviaud and Vince [1993], Ezersky *et al.* [1993], Garcimartín *et al.* [1997], Pelacho *et al.* [1999,

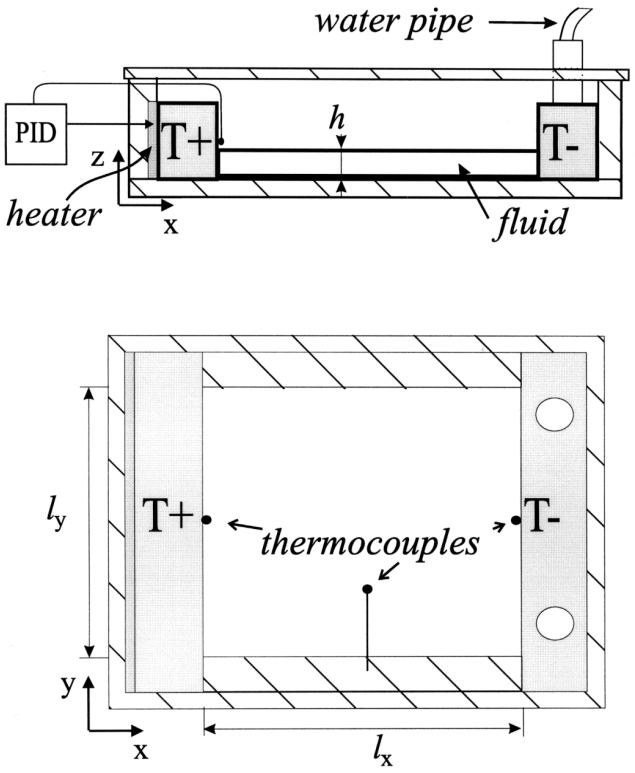

Fig. 1. Sketch of the container (side view and top view), showing the placement of the thermocouples. The geometry of the cell (both l_x and l_y) can be changed.

2000] and Burguete *et al.* [1999]. However, the characteristics of the waves (angle of propagation, wave number, frequency, etc.) and the values of the temperature difference for the threshold — the stability diagram — varied from one experiment to another.

In this work we focus on the origin of these differences using a container with variable dimensions. As it is shown in Fig. 1, the distance l_x between the walls at different temperatures, and the distance l_y between the walls at same temperature, can be changed for a constant fluid height. The aspect ratio of the container is defined as $\Gamma = l_x/l_y$. We think that the geometry of the container has a relevant influence on the mechanism and on the appearance of the hydrothermal waves. Thus, in our experiment the external parameters are the distances l_x and l_y, and the temperature difference $\Delta T = T_+ - T_-$ between the side walls. As the instability mechanism has not been yet completely explained, we hope that our study will help to understand it. In the next section the experimental setup is reported. In Sec. 3 we provide our results and the conclusions are drawn in Sec. 4.

2. Experimental Setup

The fluid used is a silicon oil of $Pr = 10$ and kinematic viscosity $\nu = 0.65$ cSt. The physical properties of the fluid remain approximately constant in the range of the applied temperatures, so that the Boussinesq approximation is valid. The fluid is placed in a container open to the air. Its height is kept constant at $h = 1.5$ mm, as measured using a micrometer with an accuracy of 10 microns. A transparent cover is placed over the container in order to reduce the evaporation of the fluid, which is about 2% in volume during the time needed to make an experimental trial.

The open container (Fig. 1) is formed by four walls. Two of the opposite walls are made of copper in order to provide a constant temperature along each one. The distance between them is called l_x. The other two opposite walls are made of Plexiglas, having a similar thermal conductivity with respect to that of the fluid. The distance between these sides is l_y. Both lengths l_x and l_y can be varied between 41 mm and 100 mm. A temperature T_+ is imposed on one of the copper walls ($x = 0$) and a temperature $T_- < T_+$ on the other wall. These temperatures are approximately symmetrical to the room temperature ($\simeq 22°$C). Thus, a temperature gradient is established along the x axis. The mass of the copper pieces is big enough to ensure that their temperature is not disturbed by the temperature oscillations of the fluid. At the bottom of the container an aluminum sheet provides an approximately linear temperature profile.

In order to measure T_+ and T_- two thermocouples are held on the inner side of the copper blocks near the fluid. A thermocouple is also placed above the fluid at the middle of the cell to monitor the room temperature. The control of T_+ and T_- was achieved as follows. Cool water coming from a thermostatic bath ($\pm 0.01°$C) is circulated inside one of the copper blocks. On the other copper block an electrical heater, glued to its outer side, is controlled by means of a PID loop (see Fig. 1). The amplitude of temperature oscillations on both sides is smaller than 0.02°C.

As it is shown in Fig. 2, a shadowgraph of the fluid is captured by a camera and stored in a computer. Spatiotemporal diagrams are made in order to obtain the main physical properties of the waves: frequency, wave number and angle of propagation. Other characteristics of the waves, such

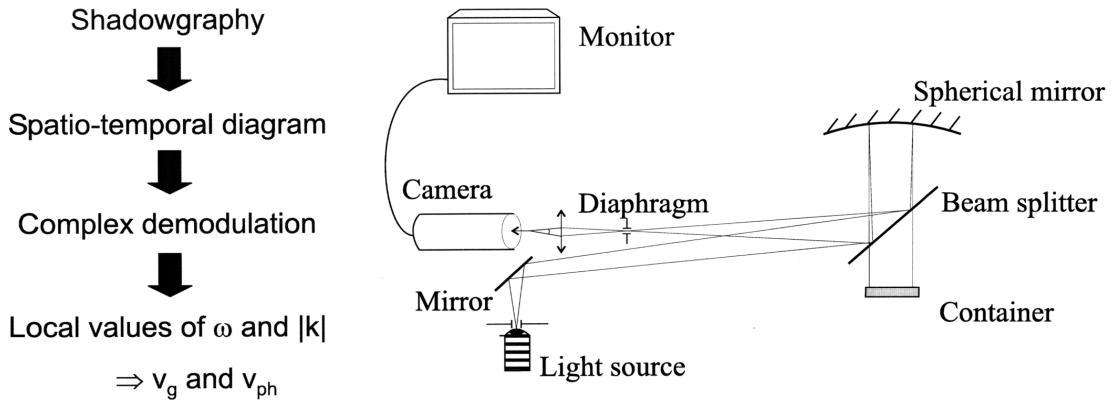

Fig. 2. Experimental setup: the shadowgraphy, along with the procedure to obtain the group (v_g) and phase (v_{ph}) velocity.

as the group velocity and the local values of the frequency and wave number, have been found using the complex demodulation technique (see [Burguete *et al.*, 1999]).

Most of the measurements of the temperature field in the fluid were obtained by introducing a thermocouple in it. This thermocouple was moved by a computer-controlled micrometric positioning system along the xyz axes. Temperature data were taken at different space and time intervals depending on whether the thermocouple was moving in the x, y or z axis. Depending on the value of l_x, 50 to 100 temperature data points are registered to obtain a good temperature profile. The time spent in each measurement is longer than the response time of the thermocouple $\tau_{\rm th} < 0.2$s. The temperature on the surface was obtained by an infrared sensor placed 10 mm above the surface.

3. Results

As it is well established, as soon as a temperature gradient is imposed along a shallow fluid layer open to the air, a flow develops in it. There is no threshold for the temperature gradient below which the fluid is at rest. Therefore the circulation is called basic flow. It consists of a single convective roll moving toward the cold wall at the surface and from the wall to the heater at the bottom. If the temperature gradient is increased, the basic flow destabilizes in a way that depends on the particular values of the parameters that define the fluid layer. A summary of them can be found in [Burguete *et al.*, 2001]. Here we choose the conditions such that the primary instability gives rise to thermocapillary waves. The features of these waves agree with the theoretical description provided by Smith and

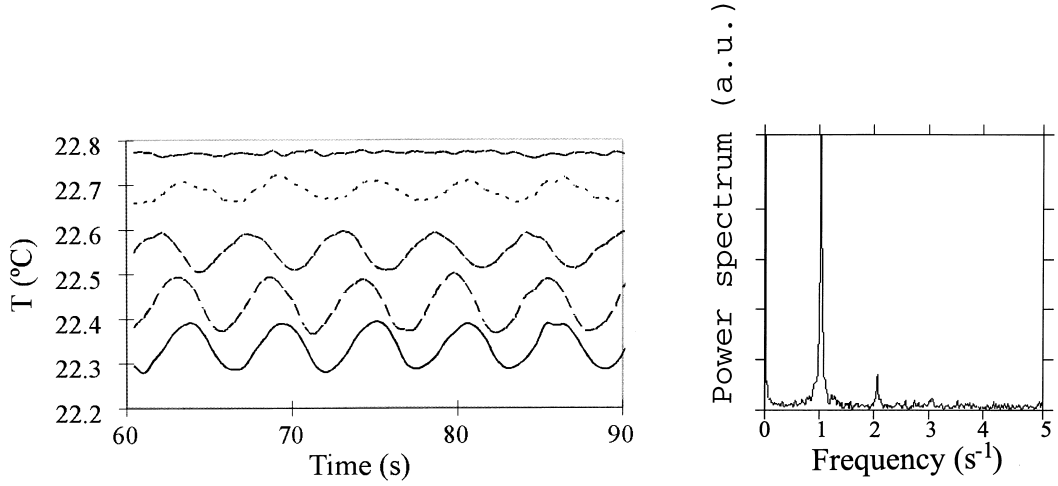

Fig. 3. (Left) Temperature oscillations versus depth for $h = 2$ mm. Each line corresponds to a different depth: from top to bottom, every 0.5 mm. The geometry of the container for which these series have been obtained is $l_x = 60$ mm and $l_y = 50$ mm. (Right) Power spectrum of the temperature oscillations for the same situation at half depth.

Davis [1983], as described elsewhere [Pelacho *et al.*, 2000]. They travel from the cold to the hot wall, at a certain angle with respect to the temperature gradient. The underlying physical process involves an interaction between the velocity field and the temperature field [Smith, 1986].

One important aspect that we have confirmed is that hydrothermal waves extend over the whole depth of the fluid layer, as opposed to surface waves. This was explained by Smith [1986]. In order to prove this, we have measured the temperature oscillations at different depths (Fig. 3). The interesting feature is that the amplitude of the waves does not decrease inside the fluid; on the contrary, waves seem to be weaker near the surface, but this may be due to heat losses to the air and no conclusive explanation can be provided at the moment.

Another piece of information that adds to the description is the variation of the wave amplitude along the direction of the temperature gradient. This can help to establish whether the instability is convective or absolute. With the dispersion relation — obtained by complex demodulation — group velocity has been determined [Pelacho *et al.*, 2000], and indeed waves travel from the cold to the hot side. As the group velocity is not zero at threshold, the instability is convective. In fact it is possible that waves are only observed after having developed to a certain point, but they could form elsewhere near the cold wall and be entrained by the flow towards the hot side. Recently, Xu and Zebib [1998] performed numerical simulations and the picture they obtain strongly suggests something similar to this scenario. We have then measured the amplitude of the waves along the x axis. As the frequency of the waves is sharply defined, we have taken the temporal series of the temperature and then calculated the peak-to-peak amplitude by Fourier analysis (Fig. 4). This was done at points spaced 1 mm in the region where waves are seen. First of all it must be noticed that from $x = 0$ to $x = 12$ mm the effects of the meniscus are not negligible; it is from $x = 12$ mm where the measurements make sense. In that region, it is seen that the amplitude of the waves grows as they travel from the cold to the hot side. The resolution of the measurements is not enough to determine the growing law. In any case, this is qualitatively similar to the results of Xu and Zebib [1998].

The fact that the amplitude of the waves grow as they approach the hot side may be related to the fact that, as we showed recently [Pelacho *et al.*, 2000], the right way to characterize the criticality is to give the *local* Marangoni number Ma_L, i.e. the Marangoni number calculated with the temperature gradient at the point considered, instead of using a mean temperature gradient. This Ma_L is not constant along the cell; instead it is bigger near the walls. The temperature profile is approximately linear at the center of the cell (Fig. 5) but near the end walls the gradient is bigger; when the temperature difference is increased, the threshold is therefore attained near the walls before than at the center.

The aim of performing this experiment in a container with variable geometry is to try to

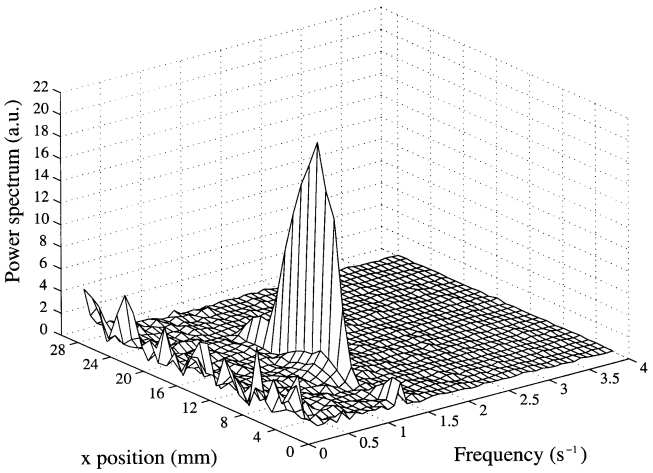

Fig. 4. Fourier spectra as a function of distance from the hot side. The maximum is obtained at 12 mm. Near the wall the waves disappear, maybe due to the meniscus.

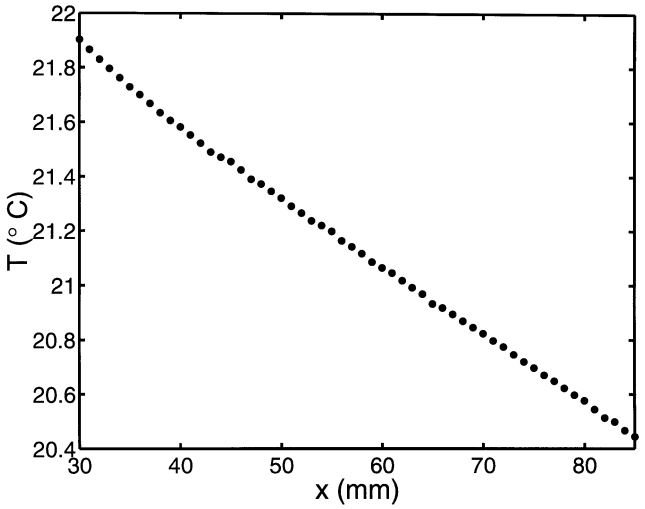

Fig. 5. Temperature profile along x at the center of the cell, obtained with an infrared sensor (sensitive to the surface temperature). Dimensions of the fluid layer are $l_x = l_y = 100$. The gradient is approximately constant.

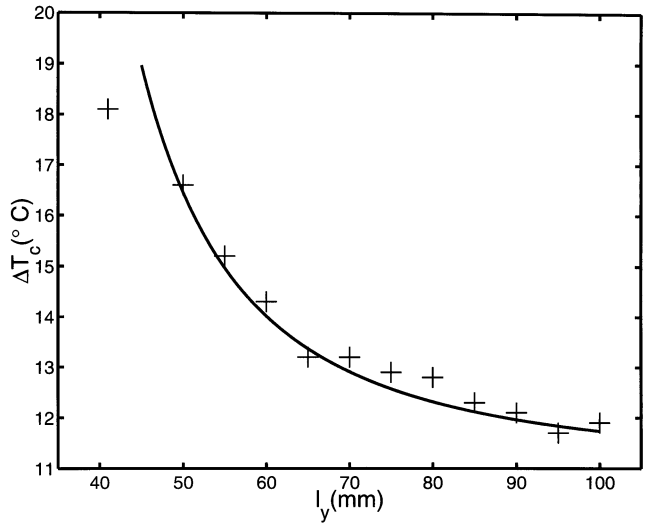

Fig. 6. The confinement effect: temperature threshold for the appearance of the waves (+) as a function of l_y, keeping $l_x = 100$. The solid line is a quadratic fit (see the text for an explanation).

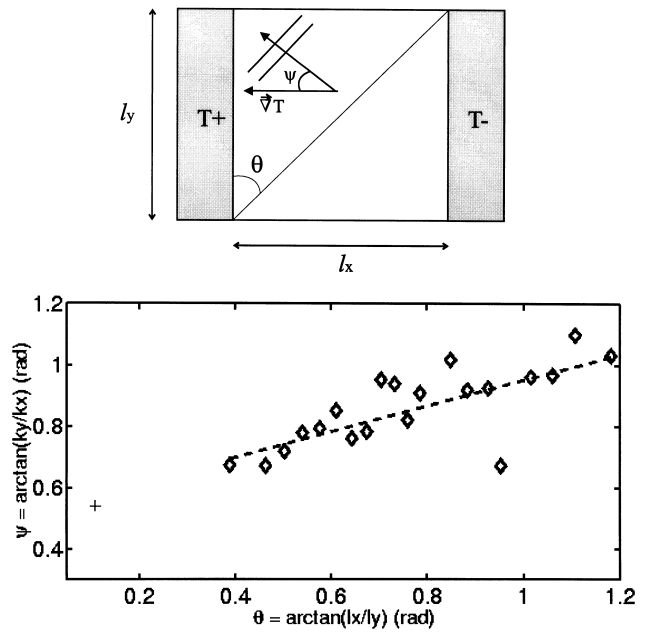

Fig. 7. The angle of propagation of the waves (Ψ) versus the angle θ, which depends on the aspect ratio l_x/l_y.

reconcile the seemingly diverging experimental results concerning the threshold for the appearance of the waves. Indeed, several authors provide different results (see [Burguete *et al.*, 2001] for a summary). The only noticeable changes are in the geometries of the containers. Besides, the threshold is calculated analytically for an infinite container. Therefore discrepancies could be explained by a finite size effect.

We have measured the threshold for the appearance of the waves changing the transversal dimension l_y. As seen in Fig. 6, there is a damping effect when l_y is small. A one-dimensional Ginzburg–Landau model gives the following law for the increase of the threshold:

$$\beta = \beta_\infty \left(1 + \frac{\xi_0^2 \pi^2}{l_y^2}\right)$$

(where β is the temperature gradient at threshold, β_∞ the gradient for an infinite system and ξ_0 the correlation length) which indeed fits well the experimental data. The increase in l_x just causes a linear increase in the threshold, as one could expect from the expression of the gradient.

The direction of propagation of the waves could also be related to the geometry. In Fig. 7 we show the angle of propagation of the waves Ψ versus the aspect ratio of the container through the variable $\theta = \arctan(l_x/l_y)$. Although the fit does not reveal a strong dependence, a trend is clear between both angles. We cannot provide a sound explanation to this fact for the moment.

4. Conclusions

We have presented experimental evidence supporting three important facts about hydrothermal waves.

Hydrothermal waves are volume waves and fill the whole depth. Their amplitude is bigger near the bottom. This result is in agreement with the theoretical results, even if the force involved is the surface-tension at the interface.

The instability is convective in nature, because of the existence of a group velocity. Consequently, the amplitude of the waves grows as they travel from the cold to the hot side. This fact makes difficult determination of the threshold, causing an overestimation.

Finally, finite size effects greatly affect the threshold and the characteristics of hydrothermal waves. The threshold increases as the transversal dimension of the fluid layer l_y decreases. This can be explained by means of simple models, as for example a Complex Ginzburg–Landau Equation. The direction of propagation of the waves depends also on the geometry of the cell. Future work will be devoted to explain this behavior.

Acknowledgments

We are indebted to François Daviaud and his colleagues of Saclay for their comments. We also thank H. L. Mancini, C. Pérez García and D. Maza for the discussions we shared. This work has been partly supported by the Spanish DGICYT contract n. PB98-0208 and by PIUNA (Universidad de Navarra). M. A. Pelacho acknowledges financial support from the "Asociación de Amigos de la Universidad de Navarra."

References

Burguete, J., Chaté, H., Daviaud, F. & Mukolobwiez, N. [1999] "Bekki–Nozaki amplitude holes in hydrothermal nonlinear waves," *Phys. Rev. Lett.* **82**, 3252–3255.

Burguete, J., Mukolobwiez, N., Daviaud, F., Garnier, N. & Chiffaudel, A. [2001] "Buoyant-thermocapillary instabilities in an extended liquid layer subjected to a horizontal temperature gradient," *Phys. Fluids* **13**, 2773–2787.

Daviaud, F. & Vince, J. M. [1993] "Traveling waves in a fluid layer subjected to a horizontal temperature gradient," *Phys. Rev.* **E48**, 4432–4436.

Ezersky, A. B., Garcimartín, A., Mancini, H. L. & Pérez-García, C. [1993] "Spatiotemporal structure of hydrothermal waves in Marangoni convection," *Phys. Rev.* **E48**, 4414–4422.

Garcimartín, A., Mukolobwiez, N. & Daviaud, F. [1997] "Origin of waves in surface-tension-driven convection," *Phys. Rev.* **E56**, 1699–1705.

Mercier, J. F. & Normand, C. [1996] "Buoyant-thermocapillary instabilities of differentially heated liquid layers," *Phys. Fluids* **8**, 1433–1445.

Parmentier, P. M., Regnier, V. C. & Lebon, G. [1993] "Buoyant-thermocapillary instabilities in medium-Prandtl-number fluid layers subject to a horizontal temperature gradient," *Int. J. Heat Mass Transf.* **36**, 2417–2427.

Pelacho, M. A. & Burguete, J. [1999] "Temperature oscillations of hydrothermal waves in thermocapillary-buoyancy convection," *Phys. Rev.* **E59**, 835–840.

Pelacho, M. A., Garcimartín, A. & Burguete, J. [2000] "Local Marangoni number at the onset of hydrothermal waves," *Phys. Rev.* **E62**, 477–483.

Smith, M. K. & Davis, S. H. [1983] "Instabilities of dynamic thermocapillary liquid layers. Part 1. Convective instabilities. Part 2. Surface-wave instabilities," *J. Fluid Mech.* **132**, 119–162.

Smith, M. K. [1986] "Instability mechanisms in dynamic thermocapillary liquid layers," *Phys. Fluids* **29**, 3182–3186.

Xu, J. & Zebib, A. [1998] "Oscillatory two- and three-dimensional thermocapillary convection," *J. Fluid Mech.* **364**, 187–209.